Engineering Science and Technology, an International Journal 18 (2015) 603–615

HOSTED BY

ELSEVIER

Contents lists available at ScienceDirect

Engineering Science and Technology, an International Journal

journal homepage: http://www.elsevier.com/locate/jestch

Full length article

Multi-objective optimization in the presence of practical constraints using non-dominated sorting hybrid cuckoo search algorithm

M. Balasubbareddy [a,*], S. Sivanagaraju [b], Chintalapudi V. Suresh [c]

[a] Department of Electrical and Electronics Engineering, Prakasam Engineering College, Kandukur, Andhra Pradesh 523105, India
[b] Department of Electrical and Electronics Engineering, University College of Engineering, JNTUK, Kakinada, Andhra Pradesh, India
[c] Research Scholar, Department of Electrical and Electronics Engineering, University College of Engineering, JNTUK, Kakinada, Andhra Pradesh, India

ARTICLE INFO

Article history:
Received 5 January 2015
Received in revised form
24 March 2015
Accepted 13 April 2015
Available online 23 May 2015

Keywords:
Hybrid cuckoo search algorithm
Non-dominated sorting
Multi-objective optimization
Generation fuel cost
Emission
Total power loss
Practical constraints

ABSTRACT

A novel optimization algorithm is proposed to solve single and multi-objective optimization problems with generation fuel cost, emission, and total power losses as objectives. The proposed method is a hybridization of the conventional cuckoo search algorithm and arithmetic crossover operations. Thus, the non-linear, non-convex objective function can be solved under practical constraints. The effectiveness of the proposed algorithm is analyzed for various cases to illustrate the effect of practical constraints on the objectives' optimization. Two and three objective multi-objective optimization problems are formulated and solved using the proposed non-dominated sorting-based hybrid cuckoo search algorithm. The effectiveness of the proposed method in confining the Pareto front solutions in the solution region is analyzed. The results for single and multi-objective optimization problems are physically interpreted on standard test functions as well as the IEEE-30 bus test system with supporting numerical and graphical results and also validated against existing methods.

1. Introduction

Due to the continuous increase in demand, research interest is focused towards the efficient operation and planning of power systems. Increased utilization and depletion of natural and fossil fuels means the research focus must include economic as well as environmental concerns. In general, the economic dispatch (ED) problem aims to increase utilization at the lowest cost of fuel.

Many classical and evolutionary approaches have been proposed to solve optimization problems with various power system objectives. Heuristic optimization techniques have been considered to solve constrained non-linear optimization problems. These methods are being used to solve problems such as economic dispatch, emission dispatch, optimal reactive power dispatch, etc. Some of the heuristic optimization techniques given in [1–26] are used to solve single objective and [27–42] to solve multi-objective optimization problems.

Recent focus has been towards economic-emission dispatch [43–49], where multi-objective evolutionary search strategies have been applied, such as non-dominated sorting genetic algorithm (NSGA) [50], Niched Pareto genetic algorithm [51], strong Pareto evolutionary algorithm [52], NSGA-II [53], multi-objective particle swarm optimization [54].

Reviewing the literature, hybridization of optimization algorithms may increase the effectiveness of an algorithm's performance. In this paper, a new algorithm is proposed incorporating arithmetic crossover into a conventional cuckoo search algorithm (CSA) [55,56], which we have called the hybrid cuckoo search algorithm (HCSA). The applicability and performance of the proposed method is analyzed in terms of convergence rate and the quality of the solution. The proposed method is validated against existing systems and is applied to solve electrical test systems with the objectives of minimizing generation fuel cost, emission, and total power loss. Non-dominated sorting-based methodology is adopted along with the proposed HCSA to solve the multi-objective optimization problem. The single and multi-objective optimization results for the electrical test systems are validated against existing literature methods. The multi-objective solution strategy is calibrated in terms of the confinement of the Pareto solutions. Finally,

* Corresponding author. Tel.:+91 9885308964; fax: +91 08598221300.
E-mail address: balasubbareddy79@gmail.com (M. Balasubbareddy).
Peer review under responsibility of Karabuk University.

http://dx.doi.org/10.1016/j.jestch.2015.04.005

we assess the effectiveness of the proposed fuzzy decision making tool in selecting the compromised solution from the best Pareto for two and three objective optimization problems. The entire methodology is tested using standard test functions and the IEEE-30 bus test system with supporting numerical and graphical results.

The optimal power flow (OPF) problem is formulated in Section 2, and various system constraints, handling of practical constraints and the conversion of constrained optimization problem to unconstrained optimization problem through penalty approach are developed. The objectives are formulated in Section 3, including the methodology related to HCSA. In Section 5, we develop the multi objective solution strategy and present the various results and analyses for standard test functions and electrical test systems in Section 6. Finally, we summarize our findings and discuss future work in Section 7.

2. Problem formulation

In general, the aim of the OPF problem is to identify a set of control variables that optimize certain power system objectives while satisfying system and practical constraints.

The OPF problem can be mathematically expressed as

$$Min\ \ A_m(x,u) \quad S.t:\ \ g(x,u) = 0\ \ and\ \ \ h(x,u) \le 0,$$

where g and h are equality and inequality constraints, respectively; x is the state vector of dependent variables, such as slack bus active power generation (P_{G1}), load bus voltage magnitudes (V_l), generator reactive power output (Q_G), and apparent power flow (S_{line}); u is the control vector of independent variables (control variables), such as the generator active power output (P_G), generator voltage (V_G), transformer tap ratios (T), and the reactive power output of shunt compensators (Q_{sh}).

The state and control vectors can be mathematically expressed as

$$x^T = \left[P_{G_1},\ V_{l_1} \dots V_{l_{NL}},\ Q_{G_1} \dots Q_{G_{NG}},\ S_{l_1} \dots S_{l_{nl}}\right]$$

$$u^T = \left[P_{G_2}\ \dots P_{G_{NG}},\ V_{G_1}\ \dots V_{G_{NG}},\ Q_{sh_1}\ \dots Q_{sh_{nc}},\ T_1\ \dots T_{nt}\right],$$

where NL, NG, nl, nc, and nt are the total number of load buses, generator buses, transmission lines, VAr sources, and regulating transformers, respectively.

The above problem is optimized satisfying the following constraints.

Equality constraints: These constraints are typically load flow equations:

$$P_{G,k} - P_{D,k} - \sum_{m=1}^{N_{bus}} |V_k||V_m||Y_{km}|\cos(\theta_{km} - \delta_k + \delta_m) = 0$$

$$Q_{G,k} - Q_{D,k} - \sum_{m=1}^{N_{bus}} |V_k||V_m||Y_{km}|\sin(\theta_{km} - \delta_k + \delta_m) = 0,$$

where P_{Gk} and Q_{Gk} are the active and reactive power generation at the kth bus, respectively; P_{Dk} and Q_{Dk} are the active and reactive power demands at the kth bus, respectively; N_{bus} is the number of buses; $|V_k|$ and $|V_m|$ are the voltage magnitudes at the kth and mth buses, respectively; δ_k and δ_m are the phase angles of the voltage at the kth and mth buses, respectively; and $|Y_{km}|$ and θ_{km} are the bus admittance magnitude and its angle between the kth and mth buses, respectively.

Inequality constraints

Generator bus voltage limits: $V_{G_i}^{\min} \le V_{G_i} \le V_{G_i}^{\max} \quad \forall\ i \in NG.$

Active Power Generation limits: $P_{G_i}^{\min} \le P_{G_i} \le P_{G_i}^{\max} \quad \forall\ i \in NG.$

Transformers tap setting limits: $T_i^{\min} \le T_i \le T_i^{\max} \quad \forall\ i \in nt.$

Capacitor reactive power generation limits: $Q_{sh_i}^{\min} \le Q_{sh_i} \le Q_{sh_i}^{\max} \quad \forall\ i \in nc.$

Transmission line flow limit: $S_{l_i} \le S_{l_i}^{\max} \quad \forall\ i \in nl.$

Reactive Power Generation limits: $Q_{G_i}^{\min} \le Q_{G_i} \le Q_{G_i}^{\max} \quad \forall\ i \in NG.$

Load bus voltage magnitude limits: $V_i^{\min} \le V_i \le V_i^{\max} \quad \forall\ i \in NL.$

Here, P_G, V_G, T, Q_{sh} inequality constraints are self restricted constraints and can be satisfied forcibly within the OPF problem, where as the remaining three constraints and active power generation at slack bus are non-self restricted constraints and these can be handled using penalty approach [1]. With this, the generalized form of the OPF problem defined as

$$A_{aug}(x,u) = A(x,u) + R_1\left(P_{G_1} - P_{G_1}^{\lim}\right)^2 + R_2\sum_{i=1}^{NL}\left(V_i - V_i^{\lim}\right)^2 + R_3\sum_{i=1}^{NG}\left(Q_{G_i} - Q_{G_i}^{\lim}\right)^2 + R_4\sum_{i=1}^{nl}\left(S_{l_i} - S_{l_i}^{\max}\right)^2$$

where R_1, R_2, R_3, andR_4 are the penalty quotients, which take large positive values. The limit values of the dependent variable $x^{\lim}$ are

$$x^{\lim} = \begin{cases} x, & x^{\min} \le x \le x^{\max} \\ x^{\max}, & x \ge x^{\max} \\ x^{\min}, & x \le x^{\min} \end{cases}$$

2.1. Practical constraints

Prohibited operating zones (POZ): In practice, when adjusting the output of a generator unit, it is important to avoid operating in prohibited zones so thermal efficiency can be maintained during vibrations in the shaft or other machine faults. This constraint can also be included in the problem formulation,

$$P_{G_i} = \begin{cases} P_{G_i}^{\min} \le P_{G_i} \le P_{G_i,1}^{L} \\ P_{G_i,k-1}^{U} \le P_{G_i} \le P_{G_i,k}^{L} & k = 2,3,\dots,n_i \\ P_{G_i,n_i}^{U} \le P_{G_i} \le P_{G_i}^{\max} \end{cases}$$

where n_i is the number of prohibited zones; k is the index of prohibited zones in unit i; and $P_{G_{i,k}}^{L}$ and $P_{G_{i,k}}^{U}$ are the lower and upper limits, respectively, of the kth prohibited zone in the ith generator.

Ramp-rate limits: The operating range of the generating units is restricted by their ramp-rate limits, which force the generators to operate continuously between two adjacent periods. The inequality constraints imposed by these ramp-rate limits are

$$\max\left(P_{G_i}^{\min}, P_{G_i}^{0} - DR_i\right) \le P_{G_i} \le \min\left(P_{G_i}^{\max}, P_{G_i}^{0} + UR_i\right)$$

where $P_{G_i}^{0}$ is the power generation of the ith unit in the previous hour, and DR_i and UR_i are the decreasing and increasing ramp-rate limits, respectively, of the ith unit.

3. Objectives formulation

We consider the objectives generation fuel cost, emission, and total power loss for analysis.

3.1. Generation fuel cost

The total generation fuel cost for NG units is

$$A_{\cos t} = \sum_{i=1}^{NG} \left(a_i P_{G_i}^2 + b_i P_{G_i} + c_i \right) \qquad \$/h, \tag{1}$$

where a_i, b_i, c_i and P_{G_i} are the fuel cost coefficients and active power generation of ith unit, respectively.

3.2. Emission

The total emission for NGunits is

$$A_{emission} = \sum_{i=1}^{NG} \left(\alpha_i P_{G_i}^2 + \beta_i P_{G_i} + \gamma_i + \varsigma_i \exp^{\lambda_i P_{G_i}} \right) \qquad ton/h, \tag{2}$$

where α_i, β_i, γ_i, ς_i, λ_i are emission coefficients of ith unit, respectively.

3.3. Total transmission loss

The total system active power loss is

$$A_{TPL} = \sum_{l=1}^{nl} g_l \left[V_i^2 + V_j^2 - 2V_i V_j \cos(\delta_i - \delta_j) \right] \qquad MW, \tag{3}$$

where, g_l is the conduction of lth line which connects buses i and j; and V_i,V_j and δ_i,δ_j are the voltage magnitude and angle of the lth and ith bus, respectively.

4. Hybrid cuckoo search algorithm (HCSA)

We develop the proposed HCSA incorporating the advantages of the CSA.

4.1. Existing cuckoo search algorithm (CSA)

CSA is a new meta-heuristic optimization method [55,56] inspired from the obligate brood parasitism of some cuckoo species by laying their eggs in the nests of other birds of other species. When the host birds discover an alien egg in their nest, they can throw it away or simply abandon their nest and build a new one elsewhere. The CSA idealized such breeding behavior in combination with Levy flights behavior of some birds and fruit flies for applying to various constrained optimization problems.

The problem control variables, u, are generated and randomly initialized between their minimum and maximum limits for a given initial population (N),

$$u_{j,i}^t = u_{j,\min} + rand_{i,j}(0,1).(u_{j,\max} - u_{j,\min}), \tag{4}$$

where, j represents the control variable in the ith population in tth iteration. Hence, the ith population in $(t+1)^{th}$ iteration is

$$u_i^{t+1} = u_i^t + S_{j,i} \times \alpha \oplus Levy(\lambda), \tag{5}$$

where, $(S_{j,i} = u_{j,i}^t - u_{best}^t)$ is the step size; $j = 1, 2, ..., m$; m is the total number of control variables; and $i = 1, 2, ..., N$. u_{best}^t is the global best solution in tth iteration. The levy flight operation is

$$Levy(\lambda) = \left| \frac{\Gamma(1+\lambda) \times \sin\left(\frac{\pi \times \lambda}{2}\right)}{\Gamma\left(\frac{1+\lambda}{2}\right) \times \lambda \times 2^{\left(\frac{\lambda-1}{2}\right)}} \right|^{1/\lambda} ; 1 < \lambda \le 3, \tag{6}$$

where, λ is the distribution factor $(0.3 \le \lambda \le 1.99)$, and $\Gamma(.)$ is the gamma distribution function.

After each iteration, the system bus and line data is updated with the new population, and load flow analysis, using the Newton Raphson (NR) method, provides the numerical solution of bus voltages, line power flows and system loss. The objectives, i.e., generation fuel cost, emission, and total power losses, are evaluated for a given population. The solution that minimizes the objective(s) is considered the best solution.

4.2. Modifications in existing CSA

Conventional optimization algorithms cannot accommodate non-linear objective functions. Meta-heuristic approaches have been developed to solve non-linear, non-continuous, and non-convex objective functions. Furthermore, hybridization has the potential to speed up exploration and find the optimum solution rapidly. Hybrid algorithms, combining two or more different methods, is a promising research field, and many satisfactory optimization results have been reported such as accuracy, convergence speed, and robustness in handling larger systems, etc. [3]. In this regard, the arithmetic crossover operation can be used to update the newly generated population and thereby the solution to speed up the convergence, which can improve exploitation of the algorithm [21].

The existing Levy flight operator in CSA can control the exploration of the solutions, to balance exploration and exploitation processes, we consider the crossover operation, which decreases the diversity of the problem and hence the final best solution will be obtained in less iterations. We call this the hybrid CSA (HCSA) optimization.

The mathematical representation of the crossover operation is [3].

$$u_{j,i}^{t+1}(new) = (1-\lambda) \times u_{best}^t + \lambda \times u_{j,i}^{t+1}, \tag{7}$$

where λ is a random number between 0 and 1. After calculating the new population using Eq. (5), this population is modified using Eq. (7). The remaining processes of identifying the best solutions from the population and calculating a new levy flight operator are then performed for a predefined number of iterations.

4.3. HCSA procedure

We present the complete implementation procedure to solve a single objective optimization problem using the proposed HCSA in the following steps.

1. Initialize the problem parameters and read the system bus, line, and OPF data.
2. Generate the initial population for the considered problem control variables using Eq. (4).
3. Update the bus and line data with the new population and perform NR load flow.
4. Evaluate the objective function (Cost, Emission, or Loss) values for the population.
5. Identify the local best solution among all solutions, and start the iterative process.

6. Update the population using Eq. (5), ensuring use of the local best solution after calculating the Levy flight operator using Eq. (6).
7. Update this new population using Eq. (7), the crossover operation.
8. Repeat the procedure, i.e. steps from 3 to 5 in each iteration and obtain the global best solution.
9. This process from steps 1-8 is continued for a predefined number of iterations.
10. After meeting the convergence criteria, output the best solution and its respective control variables.

5. Multi-objective solution strategy

The proposed HCSA may be used to solve single-objective optimization problems but is incapable of multi-objective optimization. In a multi-objective optimization, two or more objectives are solved simultaneously, while satisfying system and practical constraints using non-dominated HCSA (NSHCSA). Many optimum solutions are obtained rather than a single solution, and generally these solutions are contradictory [57].

The multi-objective optimization problem with different m objectives, which generally conflict with each other, can be formulated as

$$Minimize\ [A_1(x,u),\ A_2(x,u),\ \ldots,\ A_m(x,u)];\quad m = 1,\ 2,\ \ldots,\ m, \tag{8}$$

To perform this, the initial population is randomly generated for the considered control variables for a given population. The objective functions are evaluated and a non-dominated sorting procedure is applied on the generated solutions to obtain a Pareto front set (PFS). The best PFS is obtained using a comparison procedure. Crowding sorting is applied to sort the solutions in the

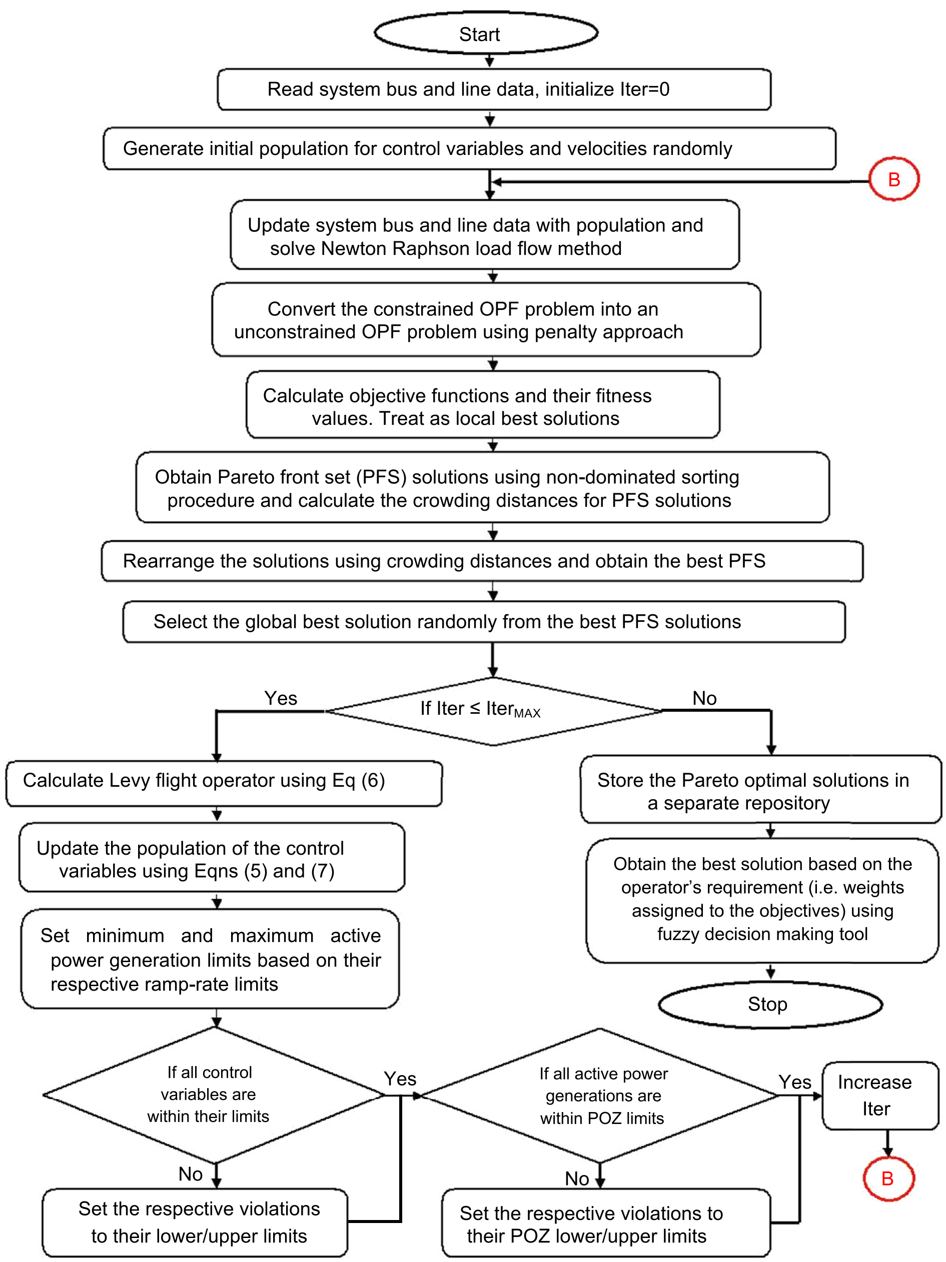

Fig. 1. Flow chart of the multi-objective solution strategy.

Table 1
Comparison of optimal parameters for Booths function.

Parameters	Existing		Proposed HCSA
	PSO	CSA	
X	1.012698676	1.002249267	1.0043728
Y	2.989245453	2.991978006	2.9969812
Function value	0.000292035	0.000202709	3.557E-05
Time (sec)	8.232991	6.95472	4.12912

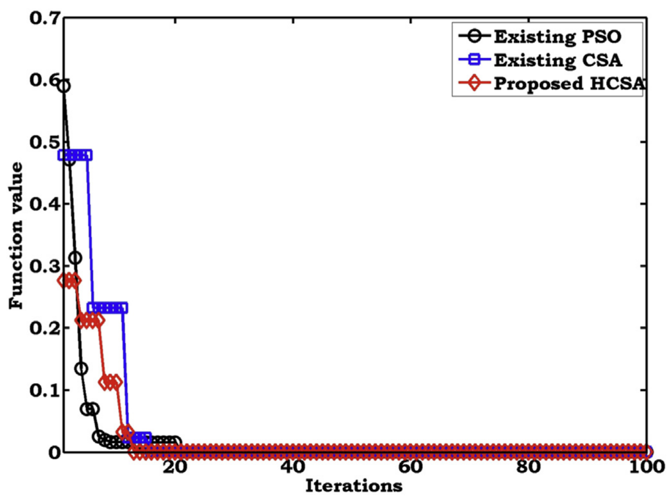

Fig. 2. Convergence characteristics of Booths function.

best PFS. Finally, a fuzzy decision making tool is applied to select the best compromised solutions as per the user requirements.

5.1. Non-dominated sorting

A non-dominated sorting procedure is applied to the multi-objective optimization solutions to obtain a PFS. Let us consider two solutions, A_1 andA_2, in one PFS. They are checked for the following possibilities: one of them dominates the other or none of them dominates each other. A vector u_1 dominatesu_2, when the following conditions are met [58].

$$\forall \quad i = 1,\ 2,\ ....,\ m, \quad A_i(u_1) \le A_i(u_2)$$
$$\exists \quad j = 1,\ 2,\ \dots,m, \quad A_j(u_1) \le A_j(u_2),$$

where, m is the total number of objective functions. Solutions that are non-dominated over the entire search space are called Pareto optimal and constitute the Pareto optimal set. We follow the sorting procedure from [59,60], based on crowding distance, to obtain the best PFS solutions.

5.2. Fuzzy decision making tool

After obtaining the best PFS solutions, we need to extract the best compromised solution based on a decision provided by the operator. We follow the fuzzy decision making mechanism proposed to obtain the optimal solution. The linear membership value, μ is initially calculated for the ith objective in the jth Pareto solution using [59,61].

$$\mu_i^j = \begin{cases} 1 & ; \quad A_i^j \le \min(A_i) \\ \dfrac{\max(A_i) - A_i^j}{\max(A_i) - \min(A_i)}; & \min(A_i) \le A_i^j \le \max(A_i) \\ 0 & ; \quad A_i^j \ge \max(A_i) \end{cases}$$

The preferred degree of the Pareto optimal solutions can be identified through normalized membership values, and this value for qth PFS solution can be calculated using

$$\mu_{opt} = \sup \frac{\sum_{p=1}^{m} W_p \mu_p^q}{\sum_{q=1}^{N_{PFS}} \sum_{p=1}^{m} W_p \mu_p^q}; \tag{9}$$

where $W_p \ge 0$; $\sum_{p=1}^{m} W_p = 1$; W_p is the weight of the pth objective function, and N_{PFS} is the total number of solutions in the best PFS. The PFS solution which has the highest normalized membership for the weight coefficients is considered to be the most optimal solution. The complete methodology of the proposed multi-objective optimization strategy is shown in Fig. 1.

6. Results and analysis

The effectiveness of the proposed methodology is tested for two examples.

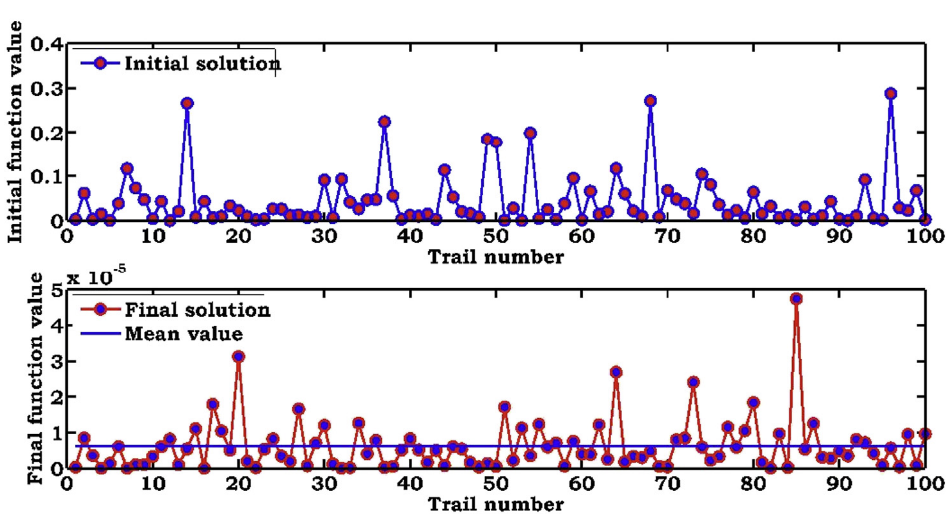

Fig. 3. Variation of the Matyas function over 100 trials using HCSA.

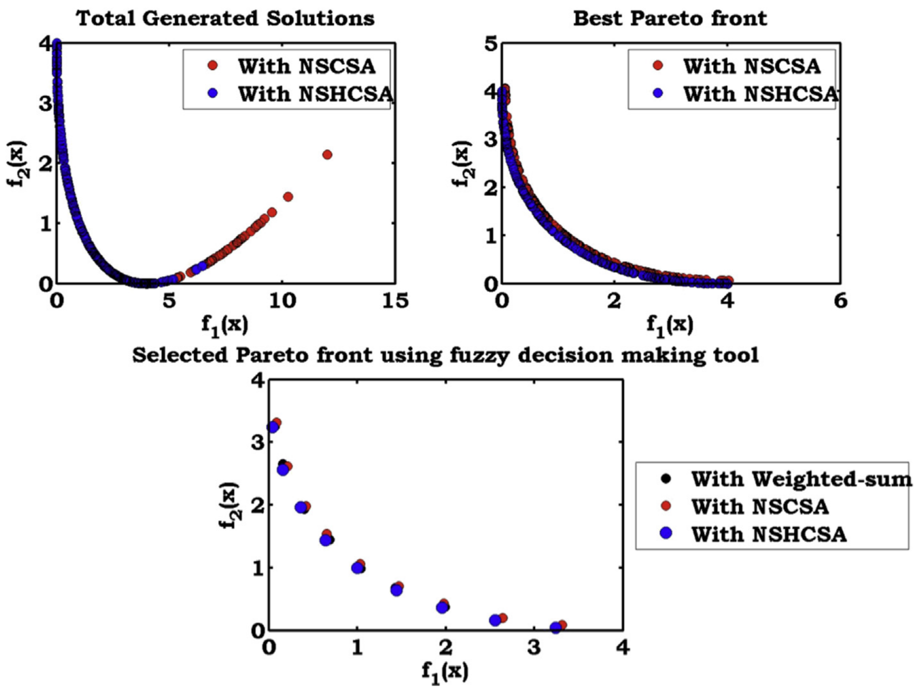

Fig. 4. Multi objective Pareto solutions for the Schaffer function.

6.1. Illustrative example

We consider Booths and Matyas functions [62] to show the effectiveness of the proposed HCSA technique over existing Particle Swarm Optimization (PSO) [10], and CSA [55] techniques in solving single objective optimization problems. The optimal parameters for the Booths function are given in Eq. (10), and the existing and proposed solution methods are shown in Table 1. The preferred solution for this function is $f(1,3)=0$ in the operating range of $-10 \le x, y \le 10$. This solution is more closely matched by the proposed HCSA compared to existing methods. Furthermore, HSCA obtains the solution in less time than the other methods.

The convergence from the different methods are shown in Fig. 2. HCSA starts with a good initial value and reaches the final best value in significantly less iterations than the other methods.

$$f(x,y) = (x+2y-7)^2 + (2x+y-5)^2 \tag{10}$$

To confirm the validity of the proposed HCSA algorithm, the Matyas function (Eq. (11)) was solved for 100 trials, and the variation of initial and final function values is shown in Fig. 3. The final function value is almost zero in all trials, and most of the final function values are below its mean value. The proposed HCSA algorithm always yields the best solution.

$$f(x,y) = 0.25\left(x^2+y^2\right) - 0.48xy \tag{11}$$

To extend the capability of the proposed NSHCSA technique to solving multi objective optimization problem, we consider the standard Schaffer (SCH) function given in functions $f_1(x)$ and $f_2(x)$ given in Eq. (12) are considered. Following the procedure of section 5, the total generated, best Pareto and selected solutions with the proposed NSHCSA and the existing NSCSA are shown in Fig. 4. The best PSF is obtained with the proposed method, and confines the entire solution region compared to existing methods.

The selected Pareto solutions obtained using the fuzzy decision making tool were also validated against the weighted sum method, as shown in Table 2. The effectiveness of the proposed fuzzy decision making tool is evident in the weight imposed on the objectives; the respective solutions are selected from the best Pareto front. The proposed NSHCSA technique yields the best results compared to existing methods.

$$Minimize = \begin{cases} f_1(x) = x^2 \\ f_2(x) = (x-2)^2 \end{cases} \tag{12}$$

Table 2
Multi-objective results for the Schaffer function.

Set No	W1	W2	Existing				Proposed NSHCSA	
			Weighted sum		NSCSA			
			F1	F2	F1	F2	F1	F2
1	0.9	0.1	0.087	3.317	0.065	3.254	0.040002	3.239978
2	0.8	0.2	0.209	2.613	0.162	2.652	0.160024	2.559905
3	0.7	0.3	0.422	1.981	0.4	1.938	0.359953	1.96011
4	0.6	0.4	0.656	1.543	0.685	1.447	0.640016	1.439976
5	0.5	0.5	1.035	1.065	1.041	0.989	1	1
6	0.4	0.6	1.472	0.702	1.433	0.675	1.440345	0.63977
7	0.3	0.7	1.974	0.425	1.987	0.377	1.959544	0.360195
8	0.2	0.8	2.643	0.202	2.583	0.174	2.559729	0.160068
9	0.1	0.9	3.313	0.087	3.249	0.061	3.239934	0.040007

6.2. Electrical test system

We consider the IEEE-30 bus test system with forty one transmission lines [63–65] to extend the features of the proposed HCSA technique to solve single objective OPF problems and proposed NSHCSA technique to solve multi-objective OPF problems. The single line diagram of the IEEE-30 bus test system is shown in Fig. 5. There are eighteen control variables for this system, which include six active power generations and respective voltage

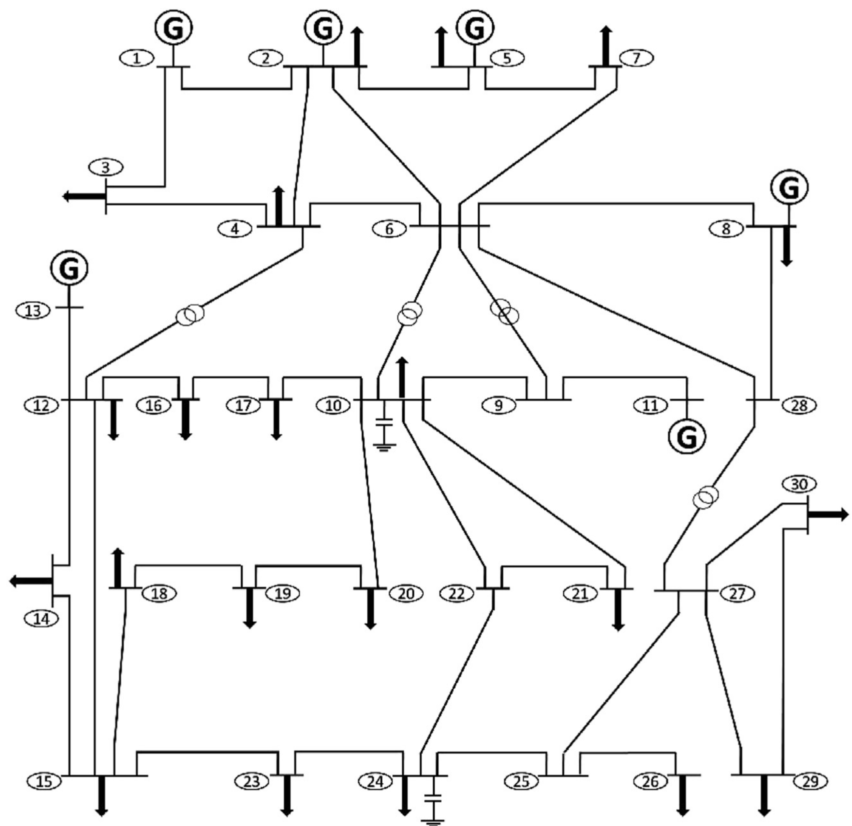

Fig. 5. Single line diagram of IEEE-30 bus system.

magnitudes, two shunt compensators and four tap setting transformers. The OPF results with generation fuel cost as an objective are shown in Table 3 for the existing and proposed methods. The proposed HCSA method produces the best generation fuel cost compared to the existing methods. The time to convergence is also less in the proposed method. To extend the validity of the results, the comparison of the obtained generation fuel cost value was compared with literature values, as shown in Table 6. This confirms that lower generation fuel cost is obtained with the proposed method. Convergence for the existing and the proposed methods are shown in Fig. 6. The proposed method starts with a good initial value and reaches the final best value in less iteration than existing methods.

Table 3
OPF results for generation fuel cost without practical constraints.

Control variables	Existing methods			Proposed HCSA
	TS [63]	PSO	CSA	
PG1(MW)	176.04	178.5558	170.7789	176.8707
PG2(MW)	48.76	48.6032	48.3696	49.88626
PG5(MW)	21.56	21.6697	18.3135	21.61352
PG8(MW)	22.05	20.7414	32.6057	20.87963
PG11(MW)	12.44	11.7702	10	11.61685
PG13(MW)	12	12	12	12
VG1(p.u.)	1.0500	1.1	1.1	1.057
VG2(p.u.)	1.0389	0.9	1.0567	1.045622
VG5(p.u.)	1.0110	0.9642	1.0912	1.018493
VG8(p.u.)	1.0198	0.9887	1.0725	1.026591
VG11(p.u.)	1.0941	0.9403	1.0465	1.057
VG13(p.u.)	1.0898	0.9284	1.1	1.057
T6–9(p.u.)	1.0407	0.9848	1.0531	1.025462
T6–10(p.u.)	0.9218	1.0299	1.007	0.972648
T4–12(p.u.)	1.0098	0.9794	1.0395	1.006042
T28–27(p.u.)	0.9402	1.0406	0.9707	0.964443
QC10(MVAr)	–	9.0931	30	25.35913
QC24(MVAr)	–	21.665	6.7556	10.6424
Total generation (MW)	292.85	293.3403	292.0677	292.867
Generation fuel cost ($/h)	802.29	803.4548	802.7283	802.0347
Emission (ton/h)	–	0.3701	0.3508	0.365688
Total power losses (MW)	–	9.9403	8.6677	9.466955
Time (sec)	–	30.2301	23.3948	17.9948

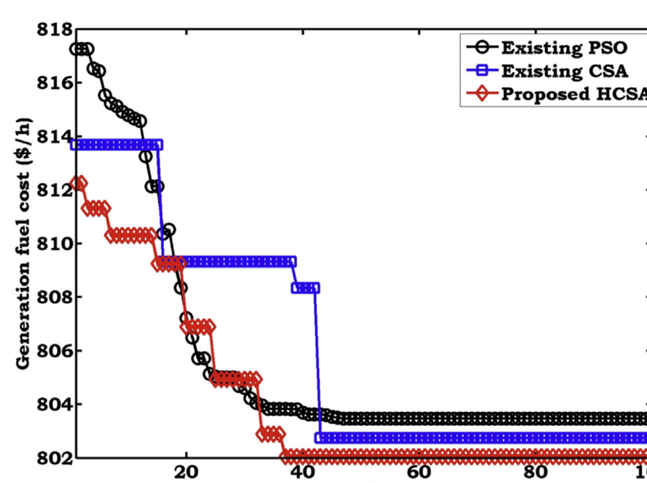

Fig. 6. Convergence for generation fuel cost.

Table 4
OPF results for generation fuel cost, emission, and total power loss objectives with and without practical constraints.

Control variables	Generation cost ($/h)				Emission (ton/h)				Total power losses (MW)			
	Case A	Case B	Case C	Case D	Case A	Case B	Case C	Case D	Case A	Case B	Case C	Case D
PG1(MW)	176.8707	176.3404	175.4662	173.5069	63.7401	82.4821	79.6604	85.7653	51.608	82.3107	51.7177	82.521
PG2(MW)	49.8863	48.279	48.3476	50	68.2844	63	60.4497	63	80	63	80	63
PG5(MW)	21.6135	21.4978	21.5623	21.5656	50	49	50	49	50	49	50	49
PG8(MW)	20.8796	19.7378	23.0082	20.271	35	30	35	30	35	30	34.9067	30
PG11(MW)	11.6169	13	12.5634	13.5283	30	28	23.3293	25	30	28	30	28
PG13(MW)	12	14	12	14	40	35	40	35	40	35	40	35
VG1(p.u.)	1.057	1.057	1.057	1.057	1.0563	1.0566	1.0466	1.057	1.057	1.057	1.057	1.057
VG2(p.u.)	1.0456	1.0443	1.0068	1.0146	1.0082	0.9876	1.0001	1.0232	1.0562	1.0529	1.0559	1.0037
VG5(p.u.)	1.0185	1.0189	1.0188	1.0151	1.0354	1.0325	1.0004	1.0392	1.0383	1.0327	1.0339	1.0324
VG8(p.u.)	1.0266	1.0304	1.0376	1.0182	1.0393	1.0307	0.986	1.057	1.0461	1.0373	1.0434	1.057
VG11(p.u.)	1.057	1.057	0.9	1.0242	1.057	1.0504	1.057	1.0188	1.057	1.0273	1.051	1.057
VG13(p.u.)	1.057	1.0332	1.057	1.057	1.0377	1.057	0.972	1.057	1.057	1.057	1.0502	0.9308
T6–9(p.u.)	1.0255	1.0354	1.019	1.0216	1.0197	0.9414	0.9	1.1	1.0134	1.0078	0.9988	0.9624
T6–10(p.u.)	0.9726	1.0621	0.923	0.9862	0.9594	1.0402	1.0324	1.0506	0.9629	0.9665	1.0117	0.9715
T4–12(p.u.)	1.006	1.0361	0.993	1.0406	0.9196	1.014	0.9	1.1	0.9802	1.0024	0.9905	0.9
T28–27(p.u.)	0.9644	0.9937	0.9705	0.9957	0.9796	0.9744	1.041	1.049	0.9654	0.9647	0.9806	0.9349
QC10(MVAr)	25.3591	25.0745	28.4048	23.0989	22.7301	13.2467	21.4139	27.1046	21.4206	20.6	18.5121	30
QC24(MVAr)	10.6424	13.8787	14.5708	18.457	24.5998	13.6385	11.0046	5	16.5347	14.2324	11.7249	16.5028
Total generation (MW)	292.867	292.855	292.9477	292.8718	287.0245	287.4821	288.4395	287.7653	286.608	287.3107	286.6244	287.521
Generation fuel cost ($/h)	802.0347	802.4735	802.9519	803.157	946.5282	913.4775	926.6635	909.1405	967.9202	913.0289	967.8243	913.5794
Emission (ton/h)	0.3657	0.3631	0.3613	0.3556	0.2048	0.2132	0.2112	0.216	0.2072	0.2131	0.2072	0.2133
Total power losses (MW)	9.467	9.455	9.5478	9.4718	3.6245	4.0821	5.0395	4.3653	3.208	3.9107	3.2244	4.121

Table 5
Ramp-rate and POZ limits followed by the generators for four cases.

Generators description	Minimization of											
	Generation cost				Emission				Total power losses			
	Case A	Case B	Case C	Case D	Case A	Case B	Case C	Case D	Case A	Case B	Case C	Case D
PG1	UP, 2	UP, 2	UP, 2	UP, 2	DOWN, 1	DOWN, 1	DOWN, 1	DOWN, 1	DOWN, 1	DOWN, 1	DOWN, 1	DOWN, 1
PG2	UP, 1	UP, 1	UP, 1	UP, 3	UP, 2	UP, 2	UP, 2	UP, 2	UP, 2	UP, 2	UP, 2	UP, 2
PG5	DOWN, 1	DOWN, 1	DOWN, 1	DOWN, 1	UP, 2	UP, 2	UP, 2	UP, 2	UP, 2	UP, 2	UP, 2	UP, 2
PG8	UP, 1	DOWN, 1	UP, 1	UP, 1	UP, 2	UP, 4	UP, 2	UP, 4	UP, 2	UP, 4	UP, 2	UP, 4
PG11	DOWN, 1	DOWN, 1	DOWN, 1	DOWN, 1	UP, 2	UP, 4	UP, 1	UP, 3	UP, 2	UP, 4	UP, 2	UP, 4
PG13	DOWN, 1	DOWN, 1	DOWN, 1	DOWN, 1	UP, 2	UP, 2	UP, 2	UP, 2	UP, 2	UP, 2	UP, 2	UP, 2

1-Below POZ lower limit; 2-Above POZ upper limit; 3-Equal to POZ lower limit; 4-Equal to POZ upper limit; UP-following up-ramp rate; DOWN-following down-ramp rate.

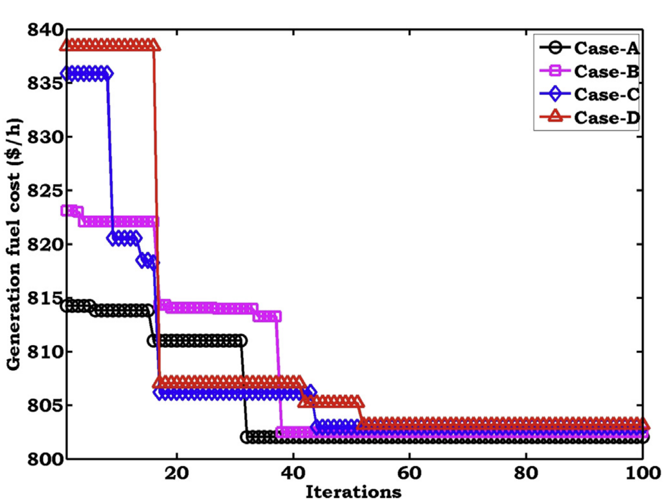

Fig. 7. Convergence of generation fuel cost for four cases.

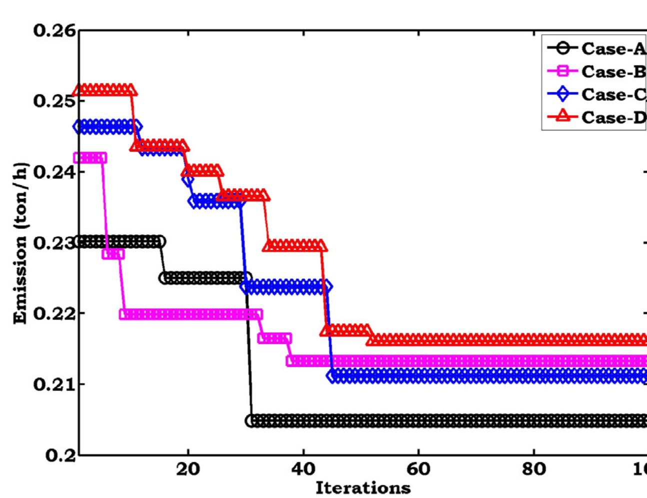

Fig. 8. Convergence of emission for four cases.

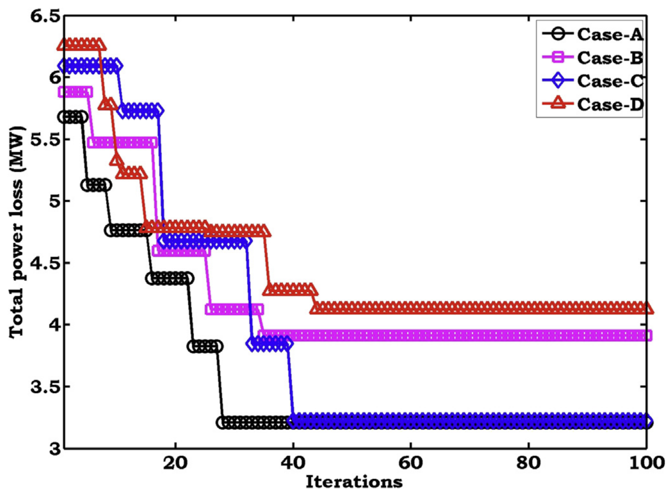

Fig. 9. Convergence of total power loss for four cases.

To show the effect of practical constraints, the OPF problem was solved for the following four cases:

- Case-A: Without ramp-rate and prohibited operating zone (POZ) limits.
- Case-B: With ramp-rate and without POZ limits.
- Case-C: Without ramp-rate and with POZ limits.
- Case-D: With ramp-rate and POZ limits.

Objectives generation fuel cost, emission, and total power losses were solved for these four cases, and the OPF results are tabulated in Table 4. As the number of constraints increase, the objective values also increase, and minimization of one objective increases the value of the other objectives. This is due to the objectives being contradictory. Due to the restrictions imposed by practical constraints on power generation, the generation is rescheduled and some generators increase and some decrease generation. Thus, the total generation and hence the total power loss also varied from case to case. Emission and total power loss objectives for Case A are shown in Table 6, and confirmed that the proposed HCSA algorithm yields superior results than existing methods.

Note that, while minimizing generation fuel cost, the slack generator is operating at higher value and the remaining generators are operating at lesser values, whereas when minimizing emission and loss objectives, this is reversed. This is because the cost coefficients are lesser and emission coefficients are higher for the slack generator. Minimizing total power losses, all generators except the slack generator are operating at respective maximum limits to decrease the power losses in transmission lines.

The ramp-rates and POZ limits followed by the generating units for the objectives in all cases are shown in Table 5. Note that all generating units are following the respective ramp-rates and are not operating in prohibited zones.

Convergence for the objectives in the four cases are shown in Figs. 7–9. The iterative process starting value and the total number of iterations taken for final convergence increase as the number of constraints increase.

The multi-objective optimization problem with two objectives was solved for the following three combinations.

- Combination-1: Generation fuel cost and Emission objectives.
- Combination-2: Generation fuel cost and Total power loss objectives.
- Combination-3: Emission and Total power loss objectives.

Following the procedure of Section 5, the total generated, best PFS, and PFS selected using the fuzzy decision making tool for the combinations are shown in Figs. 10–12. To show the effect of practical constraints on multi-objective optimization, the selected Pareto front solutions are shown without and with practical constraints. There is a significant effect from the practical constraints on objectives, and the proposed NSHCSA algorithm provides the

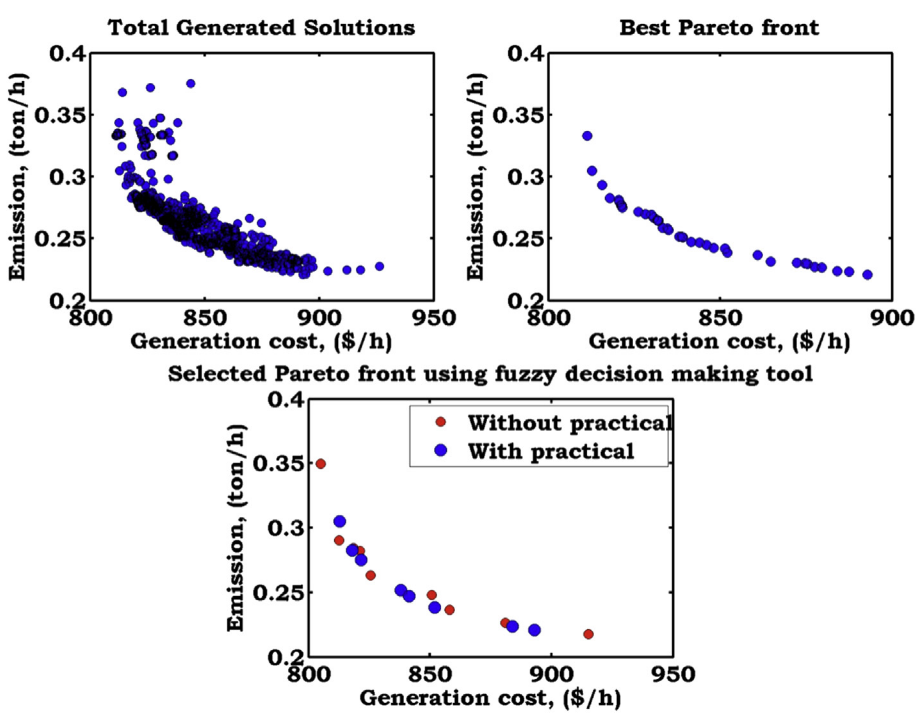

Fig. 10. Multi-objective Pareto front solutions for combination 1.

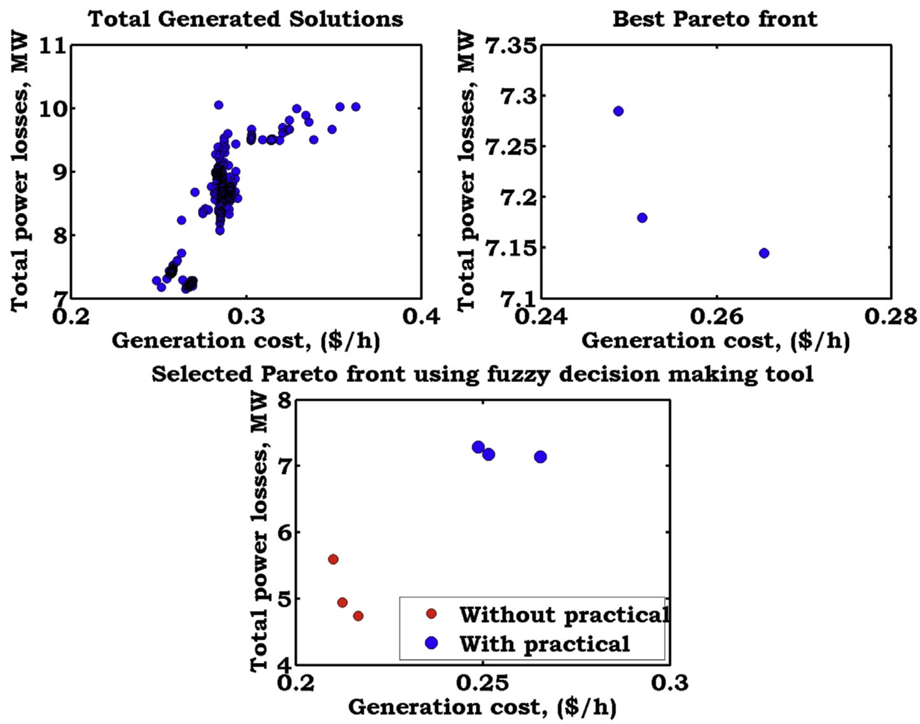

Fig. 11. Multi-objective Pareto front solutions for combination 2.

best PFS that confines the entire solutions region. The numerical results for the various weight configurations, with and without practical constraints, for the considered combinations are shown in Table 7. Based on the weights imposed on the objectives, the best compromised solution has been selected by the proposed fuzzy decision making tool. The multi-objective optimization results were further validated against existing literature outcomes, shown in Table 8. The proposed NSHCSA technique yields superior results than existing methods.

Finally, to show the extended capability of the proposed algorithm, the multi-objective optimization problem was solved considering all three objectives simultaneously. The total

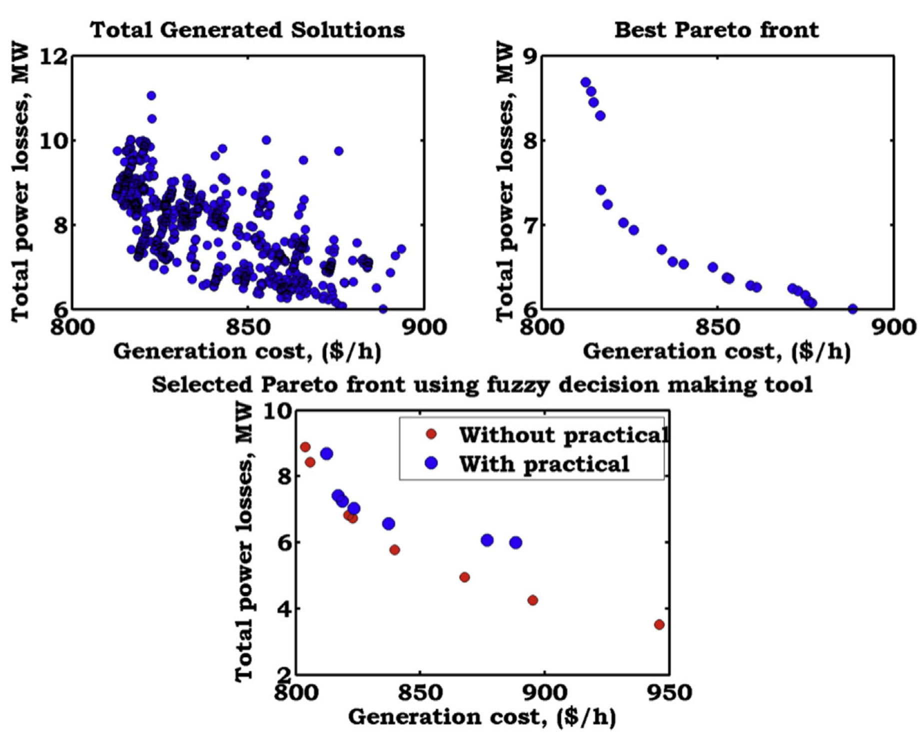

Fig. 12. Multi-objective Pareto front solutions for combination 3.

Table 6
Validation of OPF results for generation fuel cost, emission, and total power loss objectives for Cases A and D.

Methods		Generation fuel cost ($/h)	Emission (ton/h)	Total power losses (MW)
Existing	MSFLA [27]	802.287	0.2056	–
	SFLA [27]	802.5092	0.2063	–
	PSO [28]	802.190	–	3.6294
	MDE [1]	802.376	–	–
	IEP [2]	802.465	–	–
	IPSO [29]	–	0.2058	5.0732
	PSO [29]	–	0.2063	5.1204
	RGA [3]	–	–	4.57401
	CLPSO [4]	–	–	4.6282
	DE [5]	–	–	5.011
	CMAES [6]	–	–	4.945
	HSA [7]	–	–	4.9059
Proposed HCSA		802.0347	0.204823	3.208022

Table 7
Multi-objective obtained results for three combinations for Cases A and D.

Set No	W1	W2	Combination-1				Combination-2				Combination-3			
			Case A		Case D		Case A		Case D		Case A		Case D	
			COST ($/h)	EMISSION (ton/h)	COST ($/h)	EMISSION (ton/h)	COST ($/h)	LOSS (MW)	COST ($/h)	LOSS (MW)	EMISSION (ton/h)	LOSS (MW)	EMISSION (ton/h)	LOSS (MW)
1	0.9	0.1	805.0877	0.349475	812.7527	0.304942	803.6669	8.878716	812.4517	8.684898	0.200051	5.595696	0.248776	7.284695
2	0.8	0.2	811.5777	0.290295	812.7527	0.304942	805.6669	8.421013	816.8743	7.417023	0.200051	5.595696	0.251489	7.17943
3	0.7	0.3	814.3581	0.284276	817.9518	0.28272	811.0387	6.833939	818.7925	7.242575	0.200051	5.595696	0.251489	7.17943
4	0.6	0.4	821.0646	0.282075	821.5251	0.274949	812.7463	6.729621	818.7925	7.242575	0.212441	4.939599	0.251489	7.17943
5	0.5	0.5	825.4109	0.263045	838.0356	0.251677	819.5982	5.480605	823.2176	7.0247	0.212441	4.939599	0.251489	7.17943
6	0.4	0.6	850.5875	0.241178	841.5168	0.247123	867.6758	4.943254	837.226	6.562197	0.212441	4.939599	0.251489	7.17943
7	0.3	0.7	858.0959	0.236491	851.9974	0.238557	895.0949	4.257612	837.226	6.562197	0.212441	4.939599	0.265426	7.144647
8	0.2	0.8	881.0959	0.207491	883.9444	0.223556	946.0705	3.525675	876.8383	6.073851	0.216743	4.736511	0.265426	7.144647
9	0.1	0.9	915.1892	0.203633	892.8674	0.221086	946.0705	3.525675	888.285	6.0066	0.216743	4.736511	0.265426	7.144647

Table 8
Validation of Multi-objective OPF results for three combinations, Case A.

Set No	W1	W2	Combination-1				Combination-2				Combination-3	
			Case A [27]		Case A [29]		Case A [29]		Case A [28]		Case A [29]	
			COST ($/h)	EMISSION (ton/h)	COST ($/h)	EMISSION (ton/h)	COST ($/h)	LOSS (MW)	COST ($/h)	LOSS (MW)	EMISSION (ton/h)	LOSS (MW)
1	0.9	0.1	823.27788	0.2907778	–	–	–	–	–	–	–	–
2	0.8	0.2	857.40576	0.2360181	823.134	0.2751	839.843	8.976	–	–	0.2061	5.213
3	0.7	0.3	877.35636	0.2260597	–	–	–	–	–	–	–	–
4	0.6	0.4	890.54330	0.2226469	–	–	–	–	–	–	–	–
5	0.5	0.5	891.06507	0.2197379	841.052	0.2583	850.916	7.893	822.9	5.613	0.2063	5.179
6	0.4	0.6	898.49795	0.2185756	–	–	–	–	–	–	–	–
7	0.3	0.7	925.51651	0.2117979	–	–	–	–	–	–	–	–
8	0.2	0.8	942.24246	0.2107835	860.421	0.2383	869.731	6.775	–	–	0.2066	5.162
9	0.1	0.9	948.22649	0.2092571	–	–	–	–	–	–	–	–

generated, best, and selected PFS solutions, including the effect of practical constraints, are shown in Fig. 13. The best PFS obtained with the proposed method confines the entire trade off region. For this problem, there are 34 possible combinations based on the weights distribution among the objectives. For space considerations, the numerical results for nine of these combinations are given in Table 9, chosen to highlight the performance of the proposed method.

Table 9
Multi objective OPF results with three objectives.

Set No	W1	W2	W3	COST($/h)	EMISSION(ton/h)	LOSS(MW)
1	0.1	0.1	0.8	919.8273	0.262921	4.42738
2	0.1	0.8	0.1	911.2938	0.219299	4.73920
3	0.8	0.1	0.1	811.3254	0.310293	8.177524
4	0.5	0.4	0.1	823.3849	0.239384	7.394821
5	0.5	0.1	0.4	849.3023	0.252736	5.839842
6	0.4	0.5	0.1	849.3023	0.252736	5.839842
7	0.1	0.5	0.4	911.2938	0.219299	4.73920
8	0.1	0.4	0.5	911.2938	0.219299	4.73920
9	0.4	0.1	0.5	849.3023	0.252736	5.839842

7. Conclusions

A novel hybridized optimization algorithm based on the arithmetic crossover operation and conventional CSA techniques, called HCSA, was proposed. The proposed algorithm was calibrated in terms of convergence rate and the number of iterations taken for final convergence. The HCSA method was tested on standard single and multi-objective test functions and electrical test systems, to show the advantages of incorporating the crossover operation. Single objective optimization results show the proposed method enhances the performance and applicability of the convergence

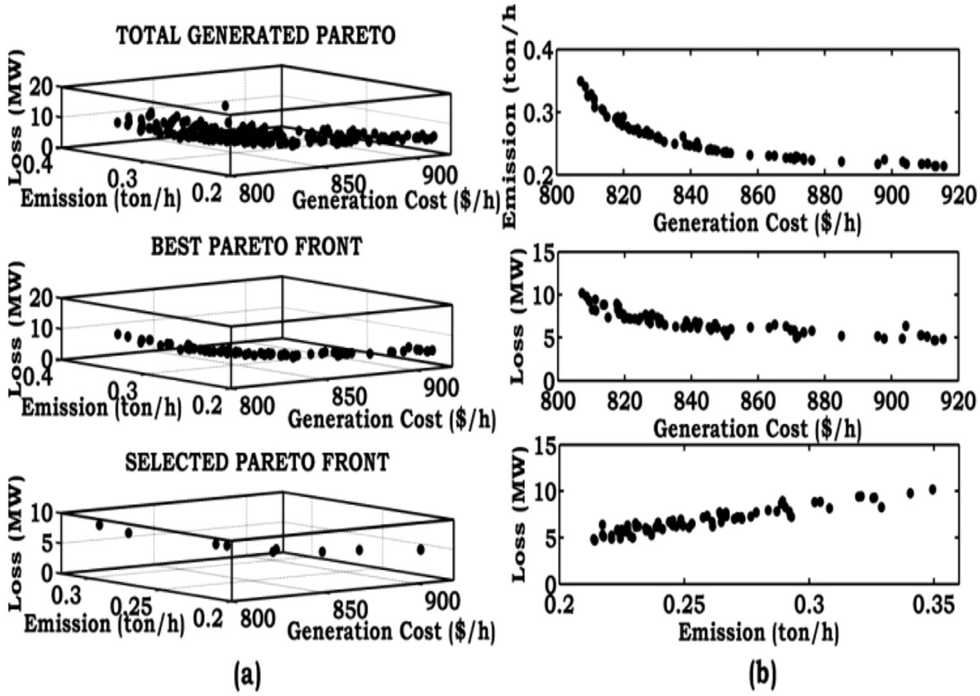

Fig. 13. Multi objective Pareto front solutions with three objectives.

and produces a superior solution compared to existing methods. The best PFS obtained with the proposed method for the multi-objective optimization problem confines the entire solutions region compared to existing methods.

The proposed new method solves single and multi-objective optimization problems with increased effectiveness for different power system objectives, such as generation fuel cost, emission, and total power loss. The effect of practical constraints on active power generation was also analyzed and the proposed HCSA method was shown to be the best when compared to existing method.

Though the proposed method is effective, the number of evolutionary operations performed during the iterative process is increased, which increases the complexity of the programming which may increase execution time. To confirm this, the future work will investigate more complicated and large scale and real time test systems.

References

[1] S. Sayah, K. Zehar, Modified differential evolution algorithm for optimal power flow with non-smooth cost functions, Energy Convers. Manag. 49 (11) (2008) 3036–3042.
[2] W. Ongsakul, T. Tantimaporn, Optimal power flow by improved evolutionary programming, Electr. Power Components Syst. 34 (1) (2006) 79–95.
[3] P. Subbaraj, P.N. Rajnarayanan, Optimal reactive power dispatch using self adaptive real coded genetic algorithm, Int. J. Electr. Power Syst. Res. 79 (2) (2009) 374–381.
[4] K. Mahadevan, P.S. Kannan, Comprehensive learning particle swarm optimization for reactive power dispatch, Appl. Soft Comput. 10 (2) (2010) 641–652.
[5] M. Varadarajan, K.S. Swarup, Differential evolution approach for optimal reactive power dispatch, Appl. Soft Comput. 8 (2008) 1549–1561.
[6] N. Hansen, CMA evolution strategy: a comparing review, Stud. Fuzziness Soft Comput. 192 (2006) 75–102.
[7] A.H. Khazali, M. Kalantar, Optimal reactive power dispatch based on harmonic search algorithm, Electr. Power Energy Syst. 33 (2011) 684–692.
[8] Ahmet H. Ertas, Optimization of fiber reinforced laminates for a maximum fatigue life by using the particle swarm optimization: part-1, Mech. Compos. Mater. 48 (6) (2013) 1011–1028.
[9] Valentina Cosentino, Salvatore Favuzza, Giorgio Graditi, Mariano, Giuseppe Ippolito, et al., Transition of a Distribution System towards an Active Network.Part-ii: Economical Analysis of Selected Scenario, ICEEP (IEEE), 2011, pp. 15–20.
[10] J. Kennedy, Eberhart Russell, Particle Swarm Optimization, IEEE International Conference on Neural Networks, 1995, pp. 1942–1948.
[11] S. Favuzza, G. Graditi, Riva, E. Sanseverino, Adaptive and dynamic ant colony search algorithm for optimal distribution systems reinforcement strategy, Appl. Intell. 24 (2006) 31–42.
[12] Maria Lusia Di Silvestre, Graditi Giorgio, Eleonora Riva Sanseverino, A generalized Framework for optimal sizing of distributed energy Resources in micro-grids using an Indicator-based swarm approach, IEEE Trans. Industrial Informatics 10 (1) (2014) 152–162.
[13] Xueming Yang, Jinsha Yuan, Jiangye Yuan, Huina Mao, A modified particle swarm optimizer with dynamic adaption, Appl. Math. Comput. 189 (2007) 1205–1213.
[14] M. Basu, Improved differential evolution for economic dispatch, Electr. Power Energy Syst. 63 (2014) 855–861.
[15] A.V. NareshBabu, T. Ramana, S. Sivangaraju, Analysis of optimal power flow problem based on two stage initialization algorithm, Electr. Power Energy Syst. 55 (2014) 91–99.
[16] Barun Mandal, Provas Kumar Roy, Sanjoy Mandal, Economic load dispatch using krill herd algorithm, Electr. Power Energy Syst. 57 (2014) 1–10.
[17] H.R.E.H. Bouchekara, M.A. Abido, M. Boucherma, Optimal power flow using teaching-learning-based optimization technique 114 (2014) 49–59.
[18] Kuntal Bhattacharjee, Aniruddha Bhattacharya, Sunita Halder nee Dey, Solution of economic load dispatch problems of power systems by real coded Chemical Reaction algorithm, Electr. Power Energy Syst. 59 (2014) 176–187.
[19] Leandro dos Santos Coelho, Teodoro Cardoso Bora, Viviana Cocco Mariani, Differential evolution based on truncated Levy-type flights and population diversity measure to solve economic load dispatch problems, Electr. Power Energy Syst. 57 (2014) 178–188.
[20] Y.Z. Li, M.S. Li, Q.H. Wu, Energy saving dispatch with complex constraints: prohibited zones, valve point effect and carbon tax, Electr. Power Energy Syst. 63 (2014) 657–666.
[21] Qun Niu, Hongyun Zhang, Xiaohai Wang, George W. Irwin, A hybrid search with arithmetic crossover operation for economic dispatch, Electr. Power Energy Syst. 62 (2014) 237–257.
[22] Vahid Hosseinnezhad, Mansour Rafiee, Mohammad Ahmadian, Mohammad Taghi Ameli, Species-based Quantum Particle Swarm Optimization for economic load dispatch, Electr. Power Energy Syst. 63 (2014) 311–322.
[23] Kuntal Bhattacharjee, Aniruddha Bhattacharya, Sunita Halder nee Dey, Oppositional real coded chemical Re- action optimization for different economic dispatch problems, Electr. Power Energy Syst. 55 (2014) 378–391.
[24] Ananthi Christry, P Ajay D Vimal Raj, Adaptive biogeography based predator-prey optimization technique for optimal power flow, Electr. Power Energy Syst. 62 (2014) 344–352.
[25] Peng Lu, Jianzhong Zhou, Huifeng Zhang, Rui Zhang, Chao Wang, Chaotic differential bee colony optimization algorithm for dynamic economic dispatch problem with valve-point effects, Electr. Power Energy Syst. 62 (2014) 130–143.
[26] Mojitaba Ghasemi, Sahand Ghavidel, Shima Rahmani, Alireza Roosta, Hasan Falah, A novel hybrid algorithm of imperialistic competitive algorithm

and teaching learning algorithm for optimal power flow problem with non-smooth cost functions, Eng. Appl. Artif. Intell. 29 (2014) 54–69.
[27] Taher Niknam, Mohammad Rasoul Narimani, Masoud Jabbari, Ahmad Reza Malekpour, A modified shuffle frog leaping algorithm for multi-objective optimal power flow, Energy 36 (2011) 6420–6432.
[28] M. Sailaja Kumari, Sydulu Maheswarapu, Enhanced Genetic Algorithm based computation technique for multi- objective optimal power flow solution, Electr. Power Energy Syst. 32 (2010) 736–742.
[29] T. Niknam, M.R. Narimani, J. Aghaei, R. Azizipanah-Abarghooee, Improved particle swarm optimization for multi- objective optimal power flow considering the cost, loss, emission and voltage stability index, IET Generation Transm. Distribution 6 (6) (2012) 515–527.
[30] M.G. Ippolito, M.L. Di Silvestre, E. Riva Sanseverino, G. Zizzo, G. Graditi, Multi-objective optimized management of electrical energy storage systems in an island network with renewable energy sources under different design scenarios, Energy 64 (2014) 648–662.
[31] Salvatore Favuzza, Giorgio Graditi, Mariano Giuseppe Ippolito, et al., Transition of a Distribution System Towards an Active Network. Part-i: Preliminary Design and Scenario Perspectives, ICEEP(IEEE), 2011, pp. 9–14.
[32] Giorgio Graditi, Maria Lusia Di Silvestre, Roberto Gallea, Eleonora Riva Sanseverino, Heuristic-based shiftable loads optimal management in smart micro-grids, IEEE Trans. Industrial Informatics 11 (1) (2015) 271–280.
[33] M.A. Abido, N.A. Al-Ali, Multi-objective optimal power flow using differential evolution, Arabian J. Sci. Eng. 37 (4) (2012) 991–1005.
[34] C.A.C. Coello, A comprehensive survey of evolutionary-based multi-objective optimization techniques, Knowl. Inf. Syst. 1 (3) (1999) 269–308.
[35] M.A. Abido, Environmental/economic power dispatch using multi-objective evolutionary algorithms, IEEE Transac. Power Syst. 18 (4) (2003) 1529–1537.
[36] K. Andrew, Z. Haiyang, Optimization of wind turbine energy and power factor with an evolutionary computation algorithm, Energy 35 (3) (2010) 1324–1332.
[37] M.A. Abido, A novel multi objective evolutionary algorithm for environmental/economic power dispatch, Electr. Power Syst. Res. 65 (2003) 71–81.
[38] Taher Niknam, Hasan Doagou Mojarrad, Bahman Bahmani Firouzi, A new optimization algorithm for multi- objective economic/emission dispatch, Electr. Power Energy Syst. 46 (2013) 283–293.
[39] Amin Shabanpour-Haghighi, Ali Reza Seifi, Taher Niknam, A modified teaching-learning based optimization for multi-objective optimal power flow problem, Energy Convers. Manag. 77 (2014) 597–607.
[40] Mojtaba Ghasemi, Sahand Ghavidel, Mohammad Mehdi Ghanbarian, Himid Reza Massrur, Masihallah Gharibzadeh, Application of imperialistic competitive algorithm with its modified techniques for multi-objective optimal power flow problem: a comparative study, Inf. Sci. 281 (2014) 225–247.
[41] Hanning Chen, Ma Lian Bo, Yunlong Zhu, Multi-hive bee foraging algorithm for multi-objective optimal power flow considering the cost, loss and emission, Electr. Power Energy Syst. 60 (2014) 203–220.
[42] B.K. Panigrahi, V. Ravikumar Pandi, Das. Sanjoy, Das Swagatam, Multiobjective fuzzy dominance based bacterial foraging algorithm to solve economic dispatch problem, Energy 35 (2010) 4761–4770.
[43] T. Niknam, R. Azizipanah-Abarghooee, M. Zare, B. Bahmani-Firouzi, Reserve constrained dynamic environmen- tal/economic dispatch: a new multi-objective self-adaptive learning bat algorithm, IEEE Syst. J. 7 (2013) 763–776.
[44] R. Azizipanah-Abarghooee, T. Niknam, A new improved bat algorithm for fuzzy interactive multi-objective eco- nomic/emission dispatch with load and wind power uncertainty, in: Uncertainty Modeling in Knowlege Engineering and Decision Making, Proceedings of the 10th International FLINS Conference, Istanbul, Turkey, 2012, p. 388.
[45] R. Azizipanah Abarghooee, J. Aghaei, Stochastic dynamic economic emission dispatch considering wind power, in: Power Engineering and Automation Conference (PEAM), IEEE, 2011, pp. 158–161.
[46] R. Azizipanah-Abarghooee, T. Niknam, M.A. Bina, M. Zare, Coordination of combined heat and power-thermal- wind-photovoltaic units in economic load dispatch using chance-constrained and jointly distributed random variables methods, Energy 79 (2015) 50–67.
[47] R. Azizipanah-Abarghooee, T. Niknam, M. Zare, M. Gharibzadeh, Multi-objective short-term scheduling of thermo- electric power systems using a novel multi-objective θ-improved cuckoo optimisation algorithm, IET Generation Transm. Distribution 8 (2014) 873–894.
[48] R. Azizipanah-Abarghooee, T. Niknam, F. Bavafa, M. Zare, Short-term scheduling of thermal power systems using hybrid gradient based modified teaching-learning optimizer with black hole algorithm, Electr. Power Syst. Res. 108 (2014) 16–34.
[49] R. Azizipanah-Abarghooee, M.R. Narimani, B. Bahmani-Firouzi, T. Niknam, Modified shuffled frog leaping algo- rithm for multi-objective optimal power flow with FACTS devices, J. Intelligent Fuzzy Syst. 26 (2014) 681–692.
[50] N. Srinivas, Deb Kalyanmoy, Multi objective optimization using non dominated sorting in genetic algorithms, Evol. Comput. 2 (3) (1994) 221–248.
[51] M.A. Abido, A niched Pareto genetic algorithm for environmental/economic power dispatch, Electr. Power Syst. Res. 25 (2) (2003) 97–105.
[52] T.F. Robert, A.H. King, C.S. Harry, Deb K. Rughooputh, Evolutionary Multi-objective Environmental/economic Dispatch: Stochastic Vs Deterministic Approaches, 2004, pp. 1–15 kanGAL Report No.2004019.
[53] S. Kannan, S. Baskar, J.D. Mccalley, P. Murugan, Application of NSGA-II algorithm to generation expansion planning, IEEE Trans. Power Syst. 24 (1) (2009) 454–461.
[54] B. Zhao, Y.J. Cao, Multiple objective particle swarm optimization technique for economic load dispatch, J. Zhejiang Univ. Sci. 6 (5) (2005) 420–427.
[55] Ehsan Afzalan, Mahmood Joorabian, An improved cuckoo search algorithm for power economic load dispatch, Int. Trans. Electr. Energy Syst. (2014), http://dx.doi.org/10.1002/etep.1878.
[56] M. Basu, A. Chowdhury, Cuckoo search algorithm for economic dispatch, Energy 60 (1) (2013) 99–108.
[57] A.A. El-Keib, H. Ma, J.L. Hart, Economic Dispatch in view of the clean AIR ACT of 1990, IEEE Trans. Power Syst. 9 (2) (1990) 972–978.
[58] T. Niknam, R. Azizipanah-Abarghooee, J. Aghaei, A new modified teaching-learning algorithm for reserve constrained dynamic economic dispatch, IEEE Trans. Power Syst. 28 (2) (2012) 749–763.
[59] K. Vaisakh, P. Praveena, S. Rama Mohana Rao, Meah Kala, Solving dynamic economic dispatch problem with security constraints using bacterial foraging PSO-DE algorithm, Electr. power energy Syst. 39 (2012) 56–67.
[60] Kalyanmoy Deb, Samir Agarwal, Amrit Pratap, T. Meyarivan, A Fast Elitist Non-dominated Sorting Genetic Algorithm for Multi-objective Optimization: NSGA-II, Kanpur Genetic Algorithms Laboratory, IIT Kanpur.
[61] J.S. Dhillon, S.C. Parti, D.P. Kothari, Stochastic economic emission load dispatch, Electr. Power Syst. Res. 26 (1993) 179–186.
[62] http://en.wikipedia.org/wiki/Test_functions_for optimization.
[63] M.A. Abido, Optimal power flow using Tabu search algorithm, Electr. power components Syst. 30 (2002) 469–483.
[64] R. Arul, G. Ravi, S. Velsami, Non-convex economic dispatch with heuristic load patterns, valve point loading effect, prohibited operating zones, ramp-rate limits, and spinning reserve constraints using harmony search algorithm, Electr. Eng. 95 (2013) 53–61.
[65] Jizhong Zhu, James A. . Momoh, Multi-area power systems economic dispatch using nonlinear convex network flow programming, Electr. Power Syst. Res. 59 (2001) 13–20.